J. Fluid Mech. (1992), *vol.* 244, *pp.* 527–546

Reynolds analogy for a shearing granular material

By DAVID G. WANG AND CHARLES S. CAMPBELL

Department of Mechanical Engineering, University of Southern California, Los Angeles, CA 90089-1453, USA

(Received 15 April 1991 and in revised form 11 May 1992)

The bulk motion of a granular material affects its apparent thermal as well as its apparent mechanical properties. This paper presents the simultaneous measurements of the apparent viscosity and thermal conductivity for a dry granular material undergoing shear in an annular shear cell. Both properties are seen to vary linearly with the shear rate. As such, it can be argued that both the apparent conductivity and viscosity are proportional to the square root of the granular temperature in exactly the same way as the kinetic theory of gases predicts that the conductivity and viscosity of a perfect gas vary as the square root of the thermodynamic temperature. Thus, analogies can be drawn between the mechanical and thermal behaviour of a granular flow that share much with similar – a.k.a. Reynolds – analogies for both laminar and turbulent flows of simple fluids. However, the results do indicate fundamental differences in the internal transport of heat and momentum. In particular, heat may only be transmitted by the streaming motion of the particles, while momentum may also be exchanged during interparticle collisions.

1. Introduction

'Reynolds analogy' for fluids is a term that is commonly used to describe relationships between their mechanical behaviour – for example the shear force exerted on a surface – and their thermal behaviour – for example the heat transfer from that surface. Such relationships exist because similar mechanisms govern the microscopic transport of both properties internal to the material. On a molecular level, the mechanism that drives the transport of both quantities is the random motion of the molecules which is characterized by the thermodynamic temperature. The macroscopic manifestations of this internal transport are the viscosity and thermal conductivity of the material. Similarly, both heat and momentum are carried by the eddies that form within a turbulent fluid, leading to the so-called 'eddy' viscosity and thermal conductivity. (It was in this context that Reynolds 1874 first proposed the analogy.) Given such strong relationships between the internal, microscopic transport of both quantities, it should not be surprising to find relationships between the resulting macroscopic surface skin friction and heat transfer.

A rapidly sheared granular material has much in common with both molecular and turbulent transport. There, collisions, induced by the shear flow, induce random motions of the particles that strongly invoke the image of the thermalized motion of molecules in the kinetic theory of gases. The image is so strong that the energy associated with the random movements is characterized as a 'granular temperature'. This has given rise to a school of thought known as rapid granular flow theory (see the review by Campbell 1990), which tries to understand the mechanics of rapidly sheared granular materials based largely on ideas derived from kinetic theory. But

unlike a real thermodynamic material, the collisions between macroscopic solid particles are inelastic. As a result, the granular temperature cannot be self-sustaining, but must be continually supplied with energy from the motion of the bulk material. Thus, like the eddies in a turbulent fluid, the granular temperature is a property of the granular flow and not a property of the granular material. And, like both the thermodynamic temperature and fluid turbulence, the random particle motions reflected in the granular temperature can induce the transport of both heat and momentum, leading one to expect that some relationship must exist between the macroscopic transport properties of both.

The literature contains several precedents for such a conclusion. For example, Patton, Sabersky & Brennen (1986) measured the friction and the heat transfer between a dry granular material and a flat plate embedded in the bottom of an inclined chute flow. They found that, as for a fluid flow, a simple relationship existed between the friction coefficient and Stanton number even though, individually, their behaviour is quite complex. A much closer relationship exists for suspensions. Leal (1973) analysed the apparent conductivity of a dilute suspension of neutrally buoyant spherical drops in the limit of low particle Reynolds (Re) and Péclet (Pe) numbers in a simple shear flow. The analysis assumed that the imposed velocity and temperature gradients both point in the same direction. In such a case, as the bulk shear motion is perpendicular to the temperature gradient, it can have no direct effect on the heat or momentum transport, so that any change in the thermal conductivity or viscosity must come from the perturbation to the fluid motion induced by the presence of the particle, or, perhaps, from the shear-induced rotation of the particle itself. Leal calculated that the shear flow enhanced the bulk thermal conductivity proportional to the $\frac{3}{2}$ power of the shear rate, a conclusion which was confirmed experimentally by Chung & Leal (1982). A similar analysis for the apparent viscosity by Lin, Peery & Schowalter (1970) showed the same $\frac{3}{2}$ power law dependence of the apparent viscosity on the shear rate, again indicating a close connection between the internal mechanisms of heat and momentum transport.

But for macroscopic materials it is possible that the mechanisms that lead to heat and momentum transport may become uncoupled. This is evident in the work of Nir & Acrivos (1976) who studied the effective thermal conductivity in the limit of low Reynolds number but large Péclet number (indicating a large-Prandtl-number fluid). In such a case, the mechanisms of momentum transport are unchanged from the case studied by Lin *et al.* (1970), but the heat transport is confined to a thin boundary layer about a closed streamline pattern that forms around the particle. In such a case, the conductivity is only weakly dependent on shear rate and varies proportional to $Pe^{1/11}$. Here, the heat and momentum transport become uncoupled as the material properties dictate that the major players in the heat transport make only a minor contribution to the momentum transport; all of the heat transport occurs within the interstitial fluid and the particle only has an influence because of the perturbation it produces within the pattern of fluid flow. This has no direct analogue for dry granular flows as, there, the thermal properties of the fluid (conductivity, heat capacity, etc.) are insignificant compared to that of the solid, and the motion of the fluid induces an insignificant amount of heat transport compared to that induced by the motion of particles. However, there still are mechanisms that contribute either to the transport of heat or to the transport of momentum without affecting the transport of the other quantity. One example, on the heat transfer side, is particle rotation. Campbell (1989) showed that, in a dry granular flow, the bulk shear motion induces a particle rotation rate of the order of one-half the shear rate – much as is observed

for particles in a fluid shear flow. By itself, the rotation of the particle does not transport linear momentum and thus cannot contribute directly to the stress. However, it does induce a convective transport of heat as a rotating particle within a temperature gradient will absorb heat on the hot side and release it on the cold side. The case of a particle rotating in a stationary medium has been studied by Wang, Sadhal & Campbell (1989), who showed that the major effect of the particle rotation is to increase the apparent conductivity of the particle relative to that of the fluid; thus, the maximum thermal conductivity of an assembly of rotating particles can be no larger than that of an assembly of stationary particles whose conductivity is infinite compared to that of the medium within which they are embedded. Thus, for a dry granular flow, as the conductivity of the solid phase is already much larger than that of the interstitial fluid, the amount of additional heat transported due to the particle rotation is insignificant.

The current study is carried out to experimentally measure the apparent thermal conductivity and the apparent viscosity of a dense dry particulate material as it undergoes shear in an annular shear cell. Here the particle concentration, particle size and shear rate are large – indicating large Re and Pe – relative to the suspension studies referred to above; as such, while there may still be a relationship between the thermal conductivity and viscosity, one should not be surprised that the low- and high-Re studies will show significantly different results. In fact, such a difference is already apparent in extensive studies of the mechanical behaviour of such systems, both by direct experimentation (Bagnold 1954; Hanes & Inman 1985; Savage & Sayed 1983) and by computer simulation (Campbell 1982, 1989; Campbell & Brennen 1985; Campbell & Gong 1986; Walton & Braun 1986*a*, *b*) (there have been no previous measurements of the thermal conductivity). The pioneering work on the constitutive behaviour of momentum transfer for granular materials was Bagnold's (1954) study of the shear flows of neutrally buoyant spherical wax particles suspended in a glycerine–water–alcohol solution. He showed that, at low shear rates, the shearing mixture behaves like a Newtonian fluid with a corrected viscosity. At large shear rates, however, the presence of the particles plays a more important role; there, the composite ceases to behave like a Newtonian fluid and the stresses, τ, vary as the square of the bulk velocity gradient according to the rule:

$$\tau = \rho_p D_p^2 f(\nu)\gamma^2, \tag{1.1}$$

where ρ_p is the density of the solid particles, D_p the particle diameter, ν the solid fraction defined as the fraction of the unit volume occupied by the solid phase, γ is the bulk shear rate and $f(\nu)$ a function of the solid fraction ν (a dimensionless density equal to the fraction of volume occupied by solid material). The same conclusion may be derived by dimensional analysis. The quadratic dependence of the stresses on the shear rate described by (1.1) has been confirmed by all of the experiments and computer simulation studies referred to above. The implication of this result is that the apparent viscosity – i.e. the shear stress divided by the shear rate – varies directly proportional to the shear rate.

2. Experimental apparatus

The apparatus used to measure the apparent conductivity is shown in figure 1. It is an annular shear cell similar to those used by Hanes & Inman (1985) and Savage & Sayed (1983) for their studies of the mechanical behaviour of sheared granular materials – although, here, the basic design has been modified so that it may

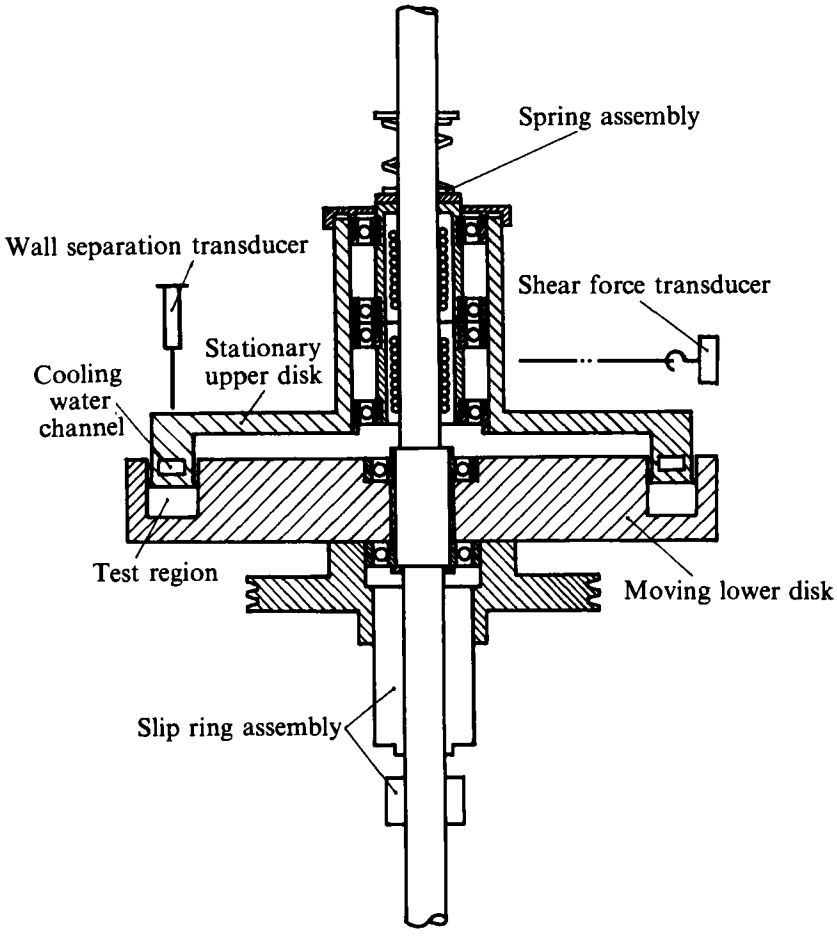

FIGURE 1. Schematic of the shear cell.

simultaneously measure the apparent conductivity. It consists of a moving lower disk and a stationary upper disk coaxially mounted on a central shaft. The lower disk is made of nylon and is 610 mm (24 in.) in diameter and 76 mm (3 in.) thick, and is mounted on a radial bearing assembly along the shaft which allows the disk to rotate freely. An annular trough of 584 mm (23 in.) in outside diameter, 483 mm (19 in.) in inside diameter and 51 mm (2 in.) deep is cut into the disk to hold the heater assembly, thermocouples and test materials. The disk is belt-driven by a 5 HP AC motor whose speed is controlled by a variable speed inverter. All of the cell's construction materials must be extremely temperature tolerant as all of the mechanical energy (up to the full 5 HP of the drive motor) is eventually dissipated away to heat and the internal temperatures may exceed 100 °C. Yet the use of metals (an obvious choice because of their resistance to abrasion and temperature) is inadvisable for the construction of the lower disk as their large thermal conductivity, relative to the test material, might bias the measurement. After several attempts, the lower disk was eventually constructed of nylon as it is able to withstand larger temperatures than many other commonly available plastics, while possessing a thermal conductivity an order of magnitude smaller than those of metals.

The upper stationary disk is made of aluminium and machined to fit closely into

the trough of the lower disk without directly contacting the trough walls. A cooling water channel is recessed right behind the surface to keep the top wall temperature constant during the heat transfer experiments. The cooling water is supplied by a Fisher Scientific constant-temperature bath. The disk is mounted on a radial-linear bearing assembly to allow free rotational and axial movement. However, rotation of the disk is prevented by a cable connected to a load cell which measures the shear force exerted on the top surface by the material. The axial movement of the top disk is restrained by a spring assembly which provides a normal force to the sheared mixture in the trough; the balance between the spring force and the shear-induced dispersive stresses controls the height of the shear gap between upper and lower disks. The gap height is monitored by a LVDT gauge head. Both the top and bottom shearing surfaces are roughened by gluing on solid particles spaced several diameters apart so that good mechanical contact is ensured between the test material and the shearing surfaces.

The heater assembly, shown in figure 2, consists of six separate heaters which are mounted behind the roughened plate that covers the trough bottom. The primary heater is located at top centre and is sandwiched by two guard heaters to prevent any heat flux through the metal plate in the direction parallel to the plate. A single ring-shaped bottom guard heater which spans the whole gap width is placed, behind a plastic spacer, at the back of the primary heater. Finally, two additional guard heaters are used to block the heat path through the sides of the plastic spacer and the roughened metal plate. To ensure that the outgoing energy from the primary heater goes nowhere but upward to the test material, the temperatures of all five guard heaters are kept the same as the temperature of the primary heater.

The measurements of temperature are made via T-type thermocouples whose positions are marked in figure 2. Three thermocouples are placed on the primary heater in order to detect any temperature gradient along its width in the radial direction. Three thermocouples are placed along each of the shearing walls and four thermocouples along the vertical sidewalls of the channel to monitor the surface temperature distribution. A total of 19 thermocouples are mounted on the rotating disk, and along with twelve leads from the heater assembly, are connected to the stationary world through two slip rings assemblies. An additional three thermocouples are attached to the stationary upper surface. For the conductivity calculation, the temperature distribution along the two roughened boundaries is determined by three thermocouples mounted flush with the outer edges of the roughened particles.

One novel feature of this device is that the shear cell is mounted inside a rotatable cage to change the orientation of the shear zone with respect to gravity. In all previous experiments that employed similar apparatuses, including Hanes & Inman (1985) and Savage & Sayed (1984), the orientation of the shear cell was fixed so that gravity worked in the same direction as the velocity gradient. Both investigators observed that, at low bulk densities, the material would gather near the trough bottom in a stagnant layer and only that portion of the material above that layer would actually shear. Consequently, they were only able to operate the experiments in a fully shearing mode at very high solid concentrations. When the present apparatus is rotated so that the shaft is parallel to the ground, gravity works perpendicular to the velocity gradient, preventing the stagnant zone formation (at least that part due to gravitational effects) and permitting operation at solid concentrations as low as 5% by volume. The stress results at low concentrations have been shown by Campbell (1986, 1990) to agree with computer simulation results

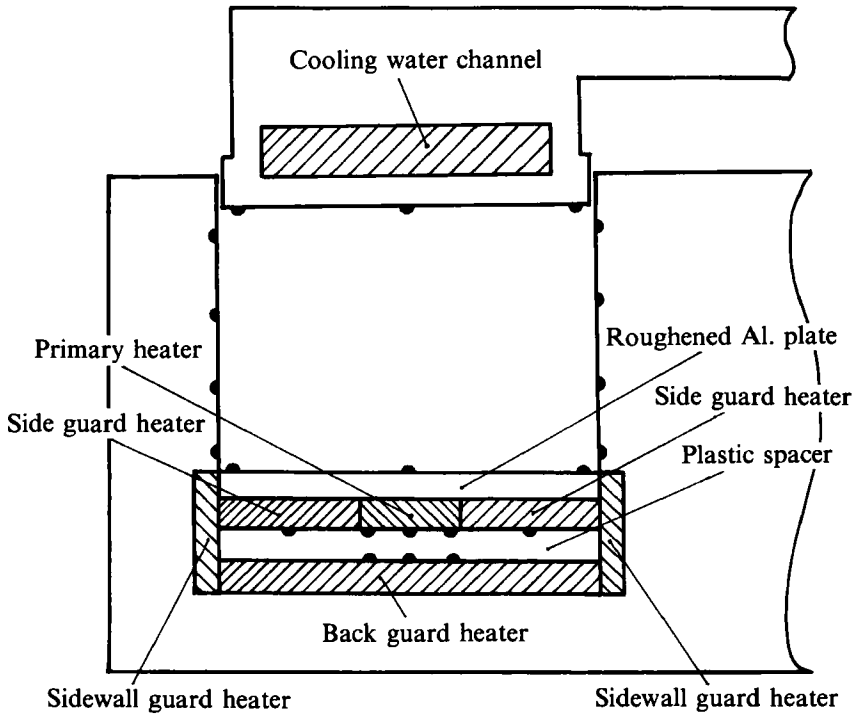

FIGURE 2. Schematic of the heater assembly and thermocouple placement.

Material	Diameter D_p (mm)	Density ρ_p (kg m^{-3})	Specific heat c_p (J kg^{-1} K^{-1})
Glass beads	1.9	2500	0.74
Steel shot	2.2	7300	0.42
Glass beads	3.0	2500	0.74
Glass beads	3.75	2500	0.74

TABLE 1. Material properties

and are the only measurements at low concentrations that do so – indicating that this is a valid method of making these measurements. In addition, the gravitational orientation varies about the circumference so that its net contribution averages to zero over a complete rotation. However, despite very successful operation at small concentrations, problems were encountered with the shear cell operated in this orientation at large concentrations. The problems appeared as vigorous oscillation of the top disk for $\nu > 0.35$. Similar oscillations are observed, though to a smaller degree, when the device was rotated into its more familiar orientation with the shaft vertical and may also be found described in the papers by Savage & Sayed and Hanes & Inman. It is speculated that at high densities, particles may percolate across the channel depth forming columns that span the gap width; as the top surface tries to move over such a column it may be temporarily lifted, as on a pole vault, generating the observed oscillation. Apparently, with the shear cell rotated so that the shaft is horizontal, there is sufficient circumferential variation in the solid concentration to promote such events (at such large concentrations, only a small perturbation would be required). One would expect that these pole vaults could transmit a force directly

from the top to the bottom disk, which might bias the force measurement and it is unclear what the consequences would be for the conductivity measurement. To minimize this problem, the shear cell is reoriented with the shaft in the vertical direction (so that gravity works parallel to the velocity gradient), whenever the concentration is larger than $\nu = 0.35$. Tests were made to assure that the orientation change did not bias either the conductivity or viscosity measurements.

Even though changing the orientation eliminates the gravity-induced formation of stagnant zones along the bottom of the channel, it is still possible for centrifugal forces to force stagnant regions to form – especially in the outside lower corners of the trough. To ensure that shearing occurs across the whole shear depth of the trough, tests are undertaken to determine the depth of the shearing for various values of solid concentration and shear rate. To accomplish this, the outer wall of the trough was covered with a layer of chalk dust. After shearing, the particles are carefully unloaded and any stagnant regions could be seen as areas where the chalk dust was undisturbed. In this way, we found that the maximum gap spacing for which no stagnant zone could be observed was about 8.5 particle diameters. As a smaller shear gap presented the danger of significant influence of the bounding walls, this spacing was used throughout the experiments described here.

Although the use of this type of device has become quite ubiquitous for granular material testing, several problems with the measurements have made themselves apparent in recent years. The most obvious problems arise from the character of the roughed boundaries. This was first noted by Hanes & Inman (1985) who performed experiments with a shear cell that was identical, in nearly every respect, to that used by Savage & Sayed (1984), except in the way that the shearing boundaries were prepared. Savage & Sayed roughened their boundaries by attaching coarse sandpaper to the shearing surfaces, while Hanes & Inman roughened theirs by gluing particles of the test material to the surfaces. Surprisingly, tests on nearly identical materials produced results that differed by a factor of up to three. Later Craig, Buckholtz & Domoto (1987) showed that the test material itself had less effect on the stress measurements than the way that the boundaries were prepared. The boundaries used in the current study were prepared by individually gluing particles spaced several diameters apart; the computer simulation results of Campbell & Gong (1987) indicate that this should provide the roughest possible boundaries, assuring good mechanical contact between the driving boundaries and the test material. In addition, Löffelmann (1989) made measurements through clear sidewalls of his shear cell and found that the generated shear rate was not uniform. Consequently, it appears that measurements made in this type of shear cell, like many rheological measurements, are device dependent and may not be quantifiably related to the properties of a material undergoing an ideal simple shearing motion.

The choice of possible test materials was extremely limited, both by constraints on size and ability to withstand the large temperatures that are generated by mechanical dissipation within the material. The maximum sizes of the particles are somewhat restricted by the maximum gap width supportable by the experimental apparatus. On the low end, the size of the particles is limited by the clearances between the stationary upper surface and the walls of the annular trough. Although originally machined to within 0.25 mm, the gap expands as the material heats until it exceeds 1 mm. This limits the size of test materials to be significantly larger than 1 mm. Furthermore, plastics are eliminated as candidates since the temperatures within the shear gap can reach 100 °C or higher. The final choices were steel shot and various sizes of glass beads whose physical properties are listed in table 1.

Further details about the design, construction and use of this apparatus, may be found in Wang (1991).

3. Experimental procedure

A typical experiment starts with a known quantity of material which is loaded into the trough in the lower disk and preheated to the temperatures that are anticipated in the experiment. The upper disk is then lowered and the orientation of the shear cell is set according to the criteria discussed in §2. The motor is started and the normal force spring is adjusted to keep constant wall separation. The shear stress, electrical power supplied to the primary heater, and the temperatures on all four bounding walls of the test region are all monitored to determine when the system reaches an equilibrium state. This process usually takes one hour, but in some cases it could take up to three hours. Many problems arose from the need to perform the experiment over such long periods of time within the highly abrasive environment of a shearing granular material.

To balance the heaters, the temperature of the primary heater is set and the power applied to the other heaters is varied until all the temperatures, measured by the appropriate thermocouples, match. Looking at figure 2, one will notice that there are three thermocouples on the primary heater, thermocouples near the outer edges of the side guard heaters and no thermocouples on the wall guard heaters. The power input to the side guard heaters was set so that the readings from the three thermocouples along the primary heater were the same. This assured that there were no temperature gradients along the surface of the primary heater that would drive heat losses in that direction. The temperature of the wall guard heaters were then set to balance the temperature of the side guard heaters.

The greatest problem arises from the abrasive wear on the roughness elements attached to the shearing surfaces. The wear makes itself apparent as a decrease in the shear stress, indicating that there may be significant slip on the shearing surfaces. Clearly, the higher the shear rate imposed on the sample and the longer the test period, the greater the damage that occurs to the roughened surfaces. Throughout this study, the experiment was stopped and the roughening particles reglued whenever a significant change in the stress was detected. At solid fractions higher than 0.40, the damage to the roughened surfaces occurred so rapidly that repair was required after each data point. As the repair requires that the experiment be shut down for a day for the glue to cure, it took a long time to perform the experiments described herein.

4. Calculation of the apparent thermal conductivity

The first step in finding the apparent thermal conductivity was to determine the temperature field, which is calculated assuming homogeneous thermal properties for the material. Afterwards, the conductivity may be easily determined from the heat supplied by the primary heater and the temperature gradient at the wall. However, for the case studied here, there are two factors that complicate such a calculation. The first problem arises because the annular region is nearly square in cross-section and significant amounts of heat may be lost through the sidewalls, resulting in a two-dimensional temperature field. In addition, the shearing process dissipates a great deal of heat and this must be taken into account in the calculation of the temperature field. Here, we make the assumption that the heat dissipation is uniformly

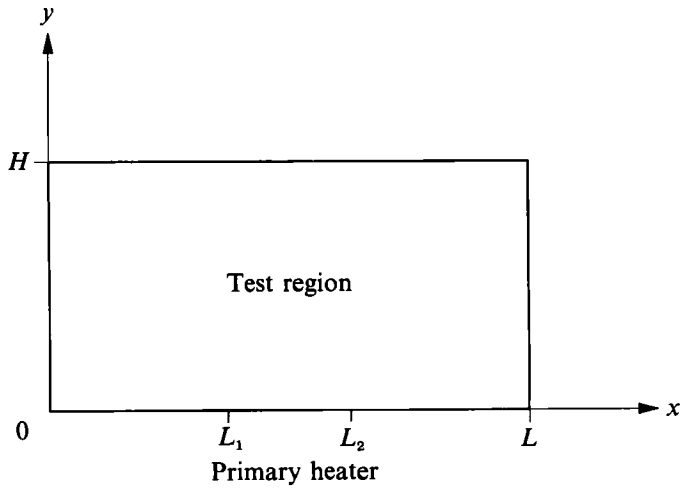

FIGURE 3. A cross-section of the annular test region upon which the conductivity calculation is performed.

distributed throughout the sample. (This is the most questionable assumption in the analysis. However, temperatures do not vary strongly along the top and bottom plates, indicating that the dissipation is, indeed, fairly uniform.) The total dissipation must equal the total work performed on the sample and is equal to SU, where S is the total shear force measured by the shear force transducer and U is the velocity of the lower plate. With these ideas in mind, the appropriate equation from which to find the temperature is

$$k\left(\frac{\partial^2 T}{\partial x^2}+\frac{\partial^2 T}{\partial y^2}\right)+\frac{SU}{V}=0, \tag{4.1}$$

where k is the apparent thermal conductivity of the shearing mixture, T is the temperature, and V the total volume of the shearing region. This calculation is done on a cross-section of the test region that is illustrated in figure 3. Here, x is the coordinate parallel to the roughened plates and varies between 0 and L, where L is the width of the annulus; y is the coordinate in the shear direction and varies between 0 and H, where H is the height of the shear gap. Equation (4.1) is to be solved subject to the boundary conditions, which are obtained by taking quadratic fits to the temperatures measured along the four walls:

$$T(x,0)=c_1x^2+b_1x+a_1 \quad \text{at} \quad y=0, \tag{4.2}$$

$$T(0,y)=c_2y^2+b_2y+a_2 \quad \text{at} \quad x=0, \tag{4.3}$$

$$T(x,H)=c_3x^2+b_3x+a_3 \quad \text{at} \quad y=H, \tag{4.4}$$

$$T(L,y)=c_4y_2+b_4y+a_4 \quad \text{at} \quad x=L, \tag{4.5}$$

with a_i, b_i, c_i being the coefficients of the quadratic fits to the temperature measurements on the boundaries. (On the top and bottom boundaries, the temperature measurement was made at the top of the roughness elements.) Now there are four thermocouples mounted on the sidewalls in the y-direction. Throughout these experiments, the gap H is varied to maintain a fixed value of H/D_p. Thus, for smaller particles, the fourth thermocouple lies outside the measurement volume and is ignored in the analysis. When all four thermocouples are within the volume, the quadratic fit is made by choosing three of the four available measurements.

Equation (4.1) is readily solved with the boundary conditions (4.2)–(4.5) by a standard separation-of-variables technique to obtain

$$T(x,y) = \sum_{n=1}^{\infty}\left[\frac{\sinh n\pi y/L}{\sinh n\pi H/L}\eta_3 + \frac{\sinh n\pi(H-y)/L}{\sinh n\pi H/L}\eta_1\right]\sin n\pi x/L$$
$$+\sum_{n=1}^{\infty}\left\{\frac{\sinh n\pi x/H}{\sinh n\pi L/H}\left[\eta_2 - \frac{2SUH^2(1-(-1)^n)}{Vk(n\pi)^3}\right]\right.$$
$$\left.+\frac{\sinh n\pi(L-x)/H}{\sinh n\pi L/H}\left[\eta_4 - \frac{2SUH^2(1-(-1)^n)}{Vk(n\pi)^3}\right] + \frac{2SUH^2(1-(-1)^n)}{Vk(n\pi)^3}\right\}\sin n\pi y/H, \tag{4.6}$$

where

$$\eta_1 = \frac{2}{n\pi}[a_1 - (c_1L^2 + b_1L + a_1)(-1)^n] - \frac{4c_1L^2}{(n\pi)^3}[1-(-1)^n],$$

$$\eta_2 = \frac{2}{n\pi}[a_2 - (c_2H^2 + b_2H + a_2)(-1)^n] - \frac{4c_2H^2}{(n\pi)^3}[1-(-1)^n],$$

$$\eta_3 = \frac{2}{n\pi}[a_3 - (c_3L^2 + b_3L + a_3)(-1)^n] - \frac{4c_3L^2}{(n\pi)^3}[1-(-1)^n],$$

$$\eta_4 = \frac{2}{n\pi}[a_4 - (c_4H^2 + b_4H + a_4)(-1)^n] - \frac{4c_4H^2}{(n\pi)^3}[1-(-1)^n].$$

Note that k is still an unknown but may be determined by realizing that the material must absorb the heat supplied by the primary heater using the temperature gradient given by the above solution, i.e.

$$\left.\frac{\partial T}{\partial y}\right|_{y=0} = -\frac{Q_{\text{wall}}}{A_0 k} \quad \text{for} \quad L_1 \leqslant x \leqslant L_2, \tag{4.7}$$

where (L_2-L_1) is the width and A_0 the surface area of the primary heater and Q_{wall} is the heat it supplies. Equations (4.6) and (4.7) may then be solved for the conductivity, k, yielding

$$k = \frac{\dfrac{4SUH^2}{V}\displaystyle\sum_{n=1}^{\infty}\frac{\cosh n\pi L_2/H - \cosh n\pi L_1/H}{\sinh n\pi L/H}\left(\frac{1-(-1)^n}{(n\pi)^3}\right) - \frac{2SUH(L_2-L_1)}{V}\sum_{n=1}^{\infty}\frac{1-(-1)^n}{(n\pi)^2} - \frac{Q_{\text{wall}}(L_2-L_1)}{A_0}}{\displaystyle\sum_{n=1}^{\infty}\left(\frac{\eta_3}{\sinh n\pi H/L} - \frac{\eta_1}{\tanh n\pi H/L}\right)(\cos n\pi L_1/L - \cos n\pi L_2/L) + \sum_{n=1}^{\infty}\frac{\cosh n\pi L_2/H - \cosh n\pi L_1/H}{\sinh n\pi L/H}(\eta_2+\eta_4)}. \tag{4.8}$$

Note that the above analysis assumes that the thermal conductivity is a scalar, which is clearly a questionable assumption. For example, Wang *et al.* (1989) have indicated that this is not the case for rotating particles. Furthermore, Campbell (1989) shows that the granular temperature is anisotropic, which, further indicates that the conductivity is not a scalar. However, despite the difficulty in solving the two-dimensional problem, the results never differ by as much as the thickness of a

data point from assuming one-dimensional conduction. This indicates minimal heat conduction in the x-direction. As symmetry dictates that there can be no conduction in the direction of flow, one can be reasonably certain that the above yields a reasonably accurate measure of the heat conduction in the y-direction.

5. Results and discussion

Results of the apparent thermal conductivity and the apparent viscosity for 3.0 mm glass beads are plotted in figures 4(*a*) and 4(*b*) as a function of shear rate for various values of solid fraction, ν. At any given value of ν, both vary linearly with the shear rate. This immediately demonstrates a relationship between the two quantities and indicates that they must have similar micromechanical underpinnings. Even more interesting is that both theoretical analysis and computer simulation have shown that, in a simple shear flow, the granular temperature varies as the square of the shear rate (see, for example, Campbell & Brennen 1985 and Lun *et al.* 1984). The same conclusion might also be drawn by simple dimensional analysis. Thus, as both the apparent thermal conductivity and the viscosity vary directly proportionally to the shear rate, they vary proportionally to the square root of the granular temperature – just as kinetic theory predicts that viscosity of a gas varies with the square root of the thermodynamic temperature. This indicates that the granular temperature governs the internal transport of both heat and momentum in a rapid granular flow.

However, the comparison between figures 4(*a*) and 4(*b*) also demonstrates a fundamental difference between the transport of heat and momentum. The slope of the apparent conductivity in figure 4(*a*) decreases with increasing solid fraction, and, at the largest solid fractions, the conductivity becomes almost independent of shear rate. Exactly the opposite behaviour is observed for the apparent viscosity shown in figure 4(*b*) in which the slopes steadily increase with solid fraction. This indicates that differences exist in the internal mechanisms that lead to the transport of heat and momentum (although, whatever the mechanism, it must still increase the transport rate proportional to the shear rate and consequently proportional to the square root of the granular temperature). Now, the internal transport of momentum is fairly well understood to occur in a combination of two modes. The collisional mode accounts for the momentum that is transferred almost instantaneously between the centres of particles during a collision and the streaming mode describes the properties carried by particles as they follow their random walk through the bulk material. Obviously, the collisional mode dominates at dense packings where collisions are frequent and the streaming mode prevails at dilute packings where particles travel great distances between collisions. Note that, as the granular temperature controls both the speed at which the particles follow their random walk and the strength and frequency of collisions, it, therefore, controls the overall transport rate regardless of the transport mode. Now it is clear that heat, as well as momentum, can be transported in the streaming mode; i.e. as a particle follows its random walk through the material, it carries its heat as well as its momentum with it. But heat transfer is a relatively slow process and it is unlikely that any significant amount of heat will be transferred between particles during the brief duration of a collision. (This intuitive notion is confirmed by the analysis of Sun & Chen 1988). Consequently, there is no analogue to the collisional mode in the internal mechanisms of thermal transport and it is reasonable to expect that the streaming mode is the dominant heat transfer mechanism within a rapidly sheared material.

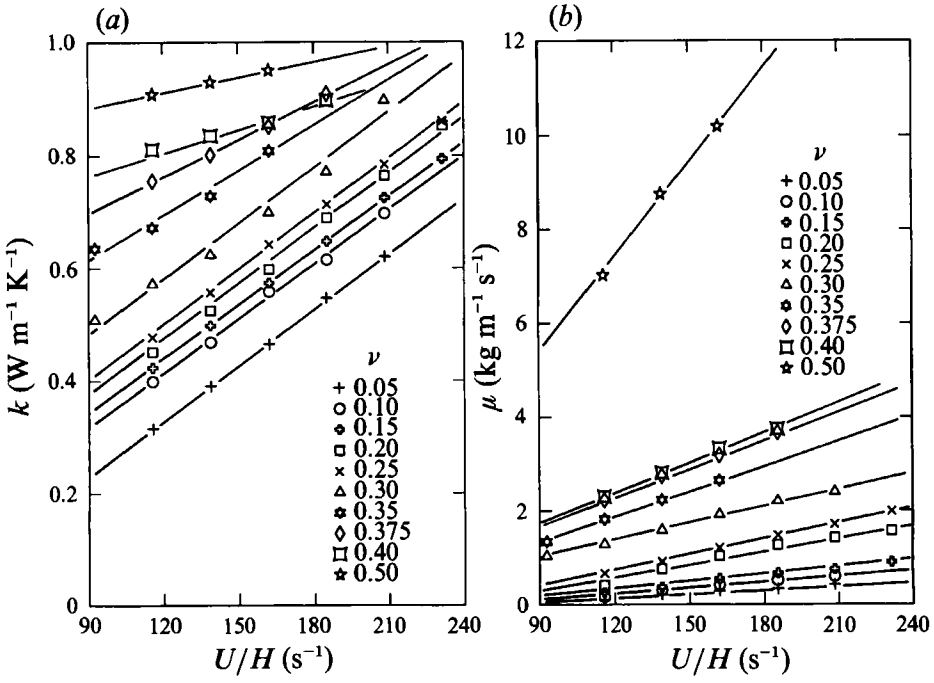

FIGURE 4. (*a*) The apparent thermal conductivity k and (*b*) the apparent shear viscosity μ as functions of shear rate for 3.0 mm glass beads.

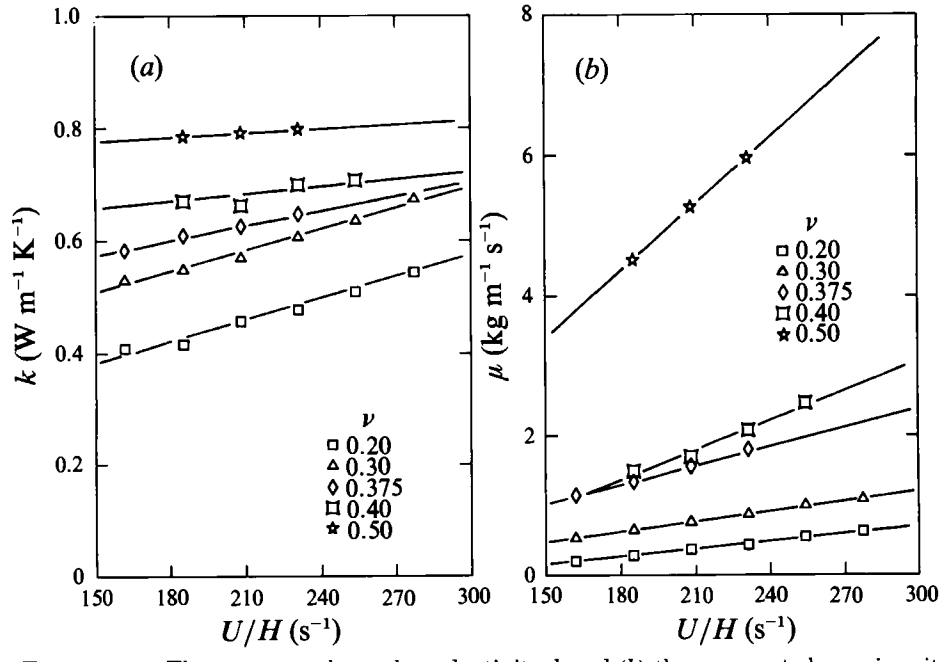

FIGURE 5. (*a*) The apparent thermal conductivity k and (*b*) the apparent shear viscosity μ as functions of shear rate for 1.9 mm glass beads.

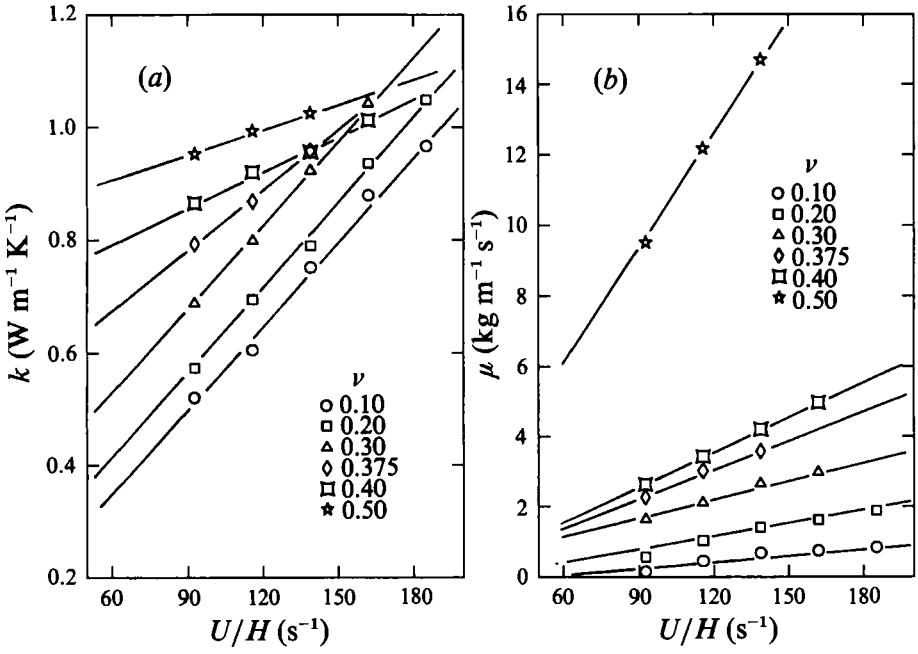

FIGURE 6. (*a*) The apparent thermal conductivity k and (*b*) the apparent shear viscosity μ as functions of shear rate for 3.75 mm glass beads.

The dominance of the streaming mode of heat transport accounts for the difference in the behaviour of the viscosity and thermal conductivity shown in figure 4. At large concentrations, the collision rate will be large, but the movement of particles is very restricted. Consequently, one anticipates a large degree of momentum transport in the collisional mode, but a reduced degree of transport of both momentum and heat in the streaming mode. The former is apparent in the increase of the slope of the viscosity lines with concentration in figure 4(*b*). However, the corresponding restriction of particle movement reduces the effectiveness of the streaming component. Regardless of the magnitude of the granular temperature (i.e. the magnitude of the shear rate) there will be no streaming momentum transport if the particles cannot move. Consequently, the larger the solid concentration, the smaller the shear-induced augmentation of the thermal conductivity, and, at the largest concentrations, the particles are essentially locked in position and the shear rate has almost no effect on the thermal conductivity. This process may be clearly seen in figure 4(*a*). Hunt & Hsiau (1990) has performed a theoretical analysis based on this same physical picture and predicts qualitatively similar results.

To check the scaling of the thermal conductivity, measurements were made for two other sizes of glass beads, 1.9 mm and 3.75 mm in diameter, and for steel shot of 2.2 mm in diameter. The results of the apparent thermal conductivity and the corresponding apparent shear viscosity measurements are shown in figures 5–7 and display much the same behaviour as the 3.0 mm glass beads shown in figure 4. As the apparent conductivities are shown to vary linearly with the shear rate for each material, density, and particle size, they can be fitted by a least squares fit into the form

$$k = k_0 + b_k \frac{U}{H}. \tag{5.1}$$

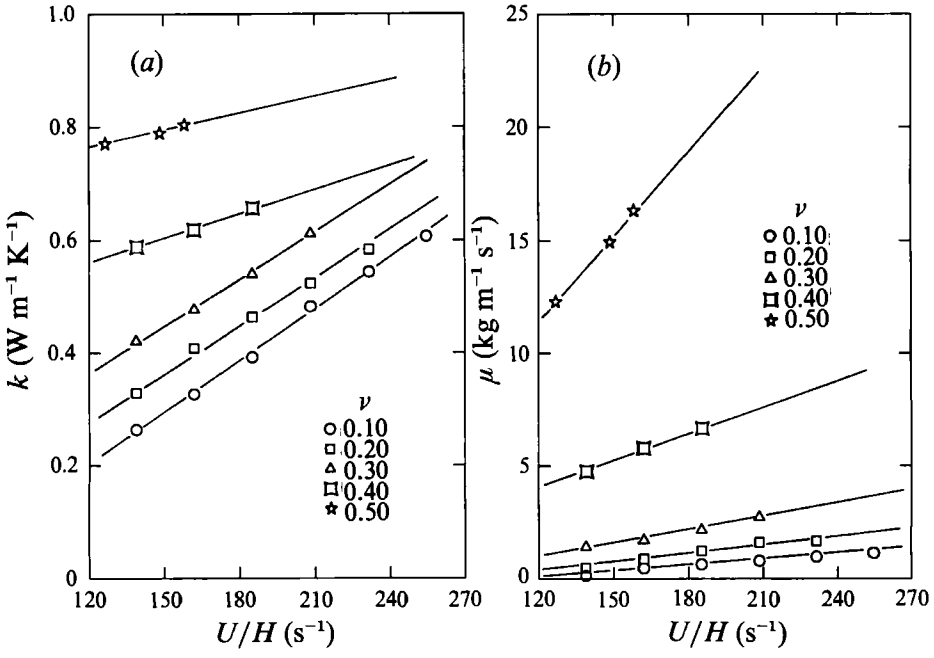

FIGURE 7. (*a*) The apparent thermal conductivity k and (*b*) the apparent shear viscosity μ as functions of shear rate for 2.2 mm steel shot.

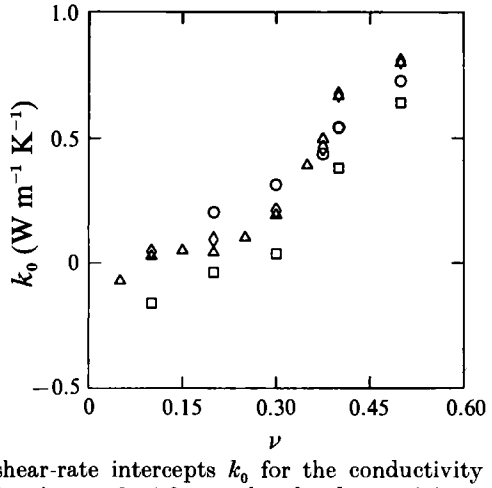

FIGURE 8. The zero-shear-rate intercepts k_0 for the conductivity measurements plotted as a function of the solid fraction ν: ○, 1.9 mm glass beads; □, 2.2 mm steel shot; △, 3.0 mm glass beads; ◇, 3.75 mm glass beads.

The values of the constant, k_0, are plotted in figure 8. Apparently, k_0 has questionable physical significance; in particular, it does not represent the conductivity of the test material in the limit of zero shear rate and, for some sets of the materials studied, even takes on negative values at the smaller solid fractions. Furthermore, at larger concentrations, k_0, takes values that are several times those that are predicted by packed-bed correlations, such as those discussed in Xavier & Davidson (1985). However, for each material, k_0 increases with solid fraction, indicating that it may still reflect the increase in apparent conductivity of

a static material as the solid fraction is increased. This might indicate that the relationship between the thermal conductivity and the shear rate is not valid down to zero shear rates. Such behaviour should not be surprising as the concept of a granular temperature, so important to the physical discussion presented above, is only appropriate for shear rates that are large enough that the stresses applied to the bulk material can be supported by the inertia of the particles (in much the same way as the pressure of a hard-sphere gas is supported by the inertia of the molecules). At small shear rates, the bulk material behaves more like a solid than a fluid and it is impossible to induce a uniform shear rate on the material. Instead, most of the material will not deform and relative motion between particles will only be evident on thin slip lines called shear bands. Under such conditions, one would be surprised if the same behaviour was apparent in the thermal conductivity at low values of shear rate as at high shear rates.

However, the diffuse nature of the $k_0(\nu)$ data may be simply due to extrapolation errors. All of the data are taken at large shear rates (90–270 s^{-1}) and the extrapolation of the curve fits down to zero shear rate is bound to introduce significant numerical errors. In itself, this may explain the scatter in the data and the strange appearance of negative values of k_0.

Since the principal internal mechanism of heat transport is by the streaming mode, i.e. the heat carried by the particles as they follow their random paths through the bulk material, one expects that the apparent conductivity should scale with the heat capacity of the particle and thus be proportional to $\rho_p c_p$. As the thermal conductivity scales with the shear rate, U/H, it follows then that the augmentation of the apparent conductivity is proportional to $\rho_p c_p(U/H)$, which bears the units of the thermal conductivity multiplied by (length)$^{-2}$. As the particle diameter D_p is the only reasonable choice for the characteristic lengthscale of microscopic transport processes, an appropriate dimensionless form of the thermal conductivity is

$$\frac{k-k_0}{\rho_p c_p D_p^2(U/H)}, \tag{5.2}$$

which dimensional analysis indicates can only be a function of the solid fraction ν. The resulting non-dimensional conductivity enhancement for all three sizes of glass beads and steel shot, is plotted in figure 9 as a function of the solid fraction ν and, encouragingly, all of the data collapse onto a single curve. It should be pointed out that the success of this collapse is, in part, because the steel and glass beads have nearly the same coefficients of restitution (measured in drop tests to be about 0.8 and 0.75 respectively) and thus dissipate granular temperature at nearly the same rate. As a consequence, both materials will generate nearly the same granular temperature at the same shear rate. If the generated granular temperatures were significantly different, the internal transport rates would simultaneously reflect the difference in the granular temperature and the difference in the specific heat of the particles and a scaling as simple as (5.2) would not be possible.

An interesting feature of this curve is that it is nearly constant over a wide range of the smaller solid fractions and only begins to drop off at the largest values of ν. While this may seem surprising at first, it has a direct analogy in the kinetic theory of gases in which the thermal conductivity of a perfect gas is found to be independent of the density. This occurs because the conductivity is a product of the number density of heat carriers and the mean free path over which they travel. Increasing the density increases the number of carriers of heat, but, simultaneously, decreases the mean free path. At small concentrations, the mean free path is inversely proportional

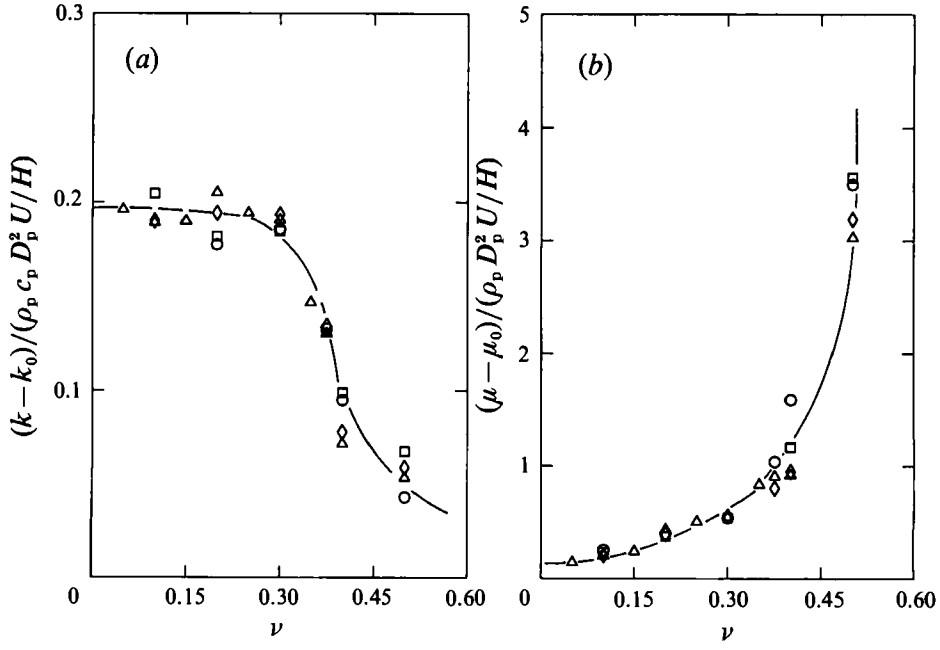

FIGURE 9. (*a*) Dimensionless conductivity augmentation as a function of solid fraction ν. (*b*) The corresponding dimensionless viscosity augmentation. Symbols as figure 8.

to the number density of carriers, so that their product and, consequently, the resulting thermal conductivity, is independent of concentration. A similar situation seems to be at work for the granular material studied here, even though a direct analogy cannot be made as there is no way to ensure that the granular temperature, which governs the transport rate, is independent of concentration in this small-ν region. A concentration dependence is visible only at very large solid fractions where the movement of particles is so restricted that they are only infrequently able to move past their neighbours. Under these conditions, one expects the mean free path to drop more rapidly than $1/\nu$, so that the dimensionless conductivity goes to zero. (This is analogous to the density correction in the Van der Waals equation of state.)

In much the same way as for the conductivity, the apparent viscosity μ for each particle size, solid fraction and material can also be fitted by a least squares method into the form

$$\mu = \mu_0 + b_\mu U/H. \tag{5.3}$$

Here, all the data extrapolate back to a non-zero value at zero shear rate for exactly the same reasons as described above for k_0, although the value of μ_0 is generally small compared to that of μ, while the value of k_0 is often comparable to that of k. By considering (1.1), a reasonable scaling of the viscosity is

$$\frac{\mu-\mu_0}{\rho_p D_p^2 (U/H)}. \tag{5.4}$$

This dimensionless group is plotted in figure 9(*b*). As might be expected from the preceding discussion, these data asymptote towards infinity at the larger values of the solid fraction. The asymptote represents the maximum concentration beyond which the material can no longer exhibit fluid-like behaviour and, like a solid, will exhibit an infinite viscosity.

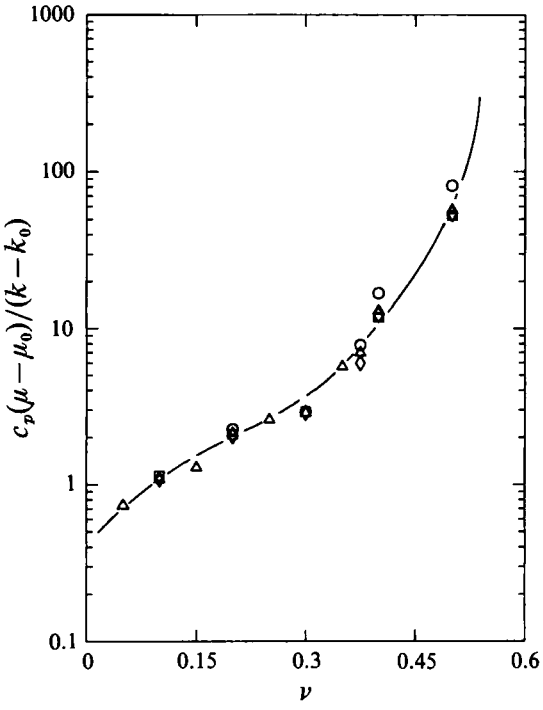

FIGURE 10. Apparent Prandtl number, $Pr = (\mu-\mu_0)c_p/(k-k_0)$, as a function of solid fraction ν. Symbols as figure 8.

The ratio of the dimensionless groups given by (5.4) and (5.2) yields the apparent Prandtl number for the shearing mixture:

$$Pr = \frac{c_p(\mu-\mu_0)}{k-k_0}. \tag{5.5}$$

Remember that the molecular and turbulent Prandtl numbers reflect the differences in the internal transport of heat and momentum. To make a direct analogy, this particular form of the Prandtl number given in (5.5) was chosen as, by subtracting away the zero intercepts, μ_0 and k_0, it reflects the differences in the shear-induced transport of heat and momentum that are the major topic of this paper. This Prandtl number is plotted in figure 10 and can be seen to be a well-defined function of the solid fraction ν. This indicates that the shear-induced transport rates of heat and momentum are related through the solid concentration and a single material property, the specific heat of the solid phase, c_p. Remember that the majority of the heat is carried by particles, in the streaming mode, as they follow their random paths through the bulk material. Thus, the heat transport rate is proportional to the heat capacity of the particles which is equal to the mass of the particle multiplied by its specific heat c_p, while the momentum transport is carried by the inertia of the particles and is therefore proportional only to the particle mass. Consequently, the dependence on mass disappears when taking the ratio that forms the Prandtl number, and leaves the specific heat as the sole remaining material property. The dependence on the solid concentration ν reflects the fact that while both collisional and streaming modes contribute to the overall momentum transfer, only the streaming mode is important in the heat transfer process.

One of the reviewers asked about the effects of the annular flow configuration on the results. The results are interpreted as if they come from an infinite shear flow yet may be dominated by a variety of undesirable ramifications of approximating the infinite flow field by a rotational system. Two possibilities were suggested. The first was simple centrifugal forces, which, if comparable to the dispersive forces generated within the material, may alter the distribution of the granular material within the channel. A more complicated problem arises from the secondary flows characteristic of the annular configuration that were reported by Savage & Sayed (1984). These are generated because, near the stationary wall, the particles will also be nearly stationary and thus experience no centrifugal forces, while, near the rotating wall, the particles will have maximum velocity and maximum centrifugal forces. Assuming that the flowing granular material behaves approximately as a fluid, this would make the pressure near the inner wall a maximum near the upper surface and a minimum near the bottom. This results in a vortical motion in the shear gap generated primarily by the pressure gradient at the inner wall between the top and bottom of the channel. While it is possible to evaluate the relative magnitude of the centrifugal forces to the dispersive stresses, the effect on the results cannot be easily quantified; i.e. are these second-order effects that can be simply ignored? At the same time, neither the velocity, nor (to an even greater extent) the contribution of the vortical motions have been quantifiably evaluated; one would expect that these would make a significant contribution to the transport properties only if the induced velocities were of the same order as the granular temperature. Without any quantitative prediction of their significance, one can only appeal to the results. In the first case, any error depends on the relative magnitude of the dispersive to centrifugal forces. But the dispersive stresses vary as the square of the particle size, while the centrifugal forces are independent of particle size. Thus, one would expect that the larger the particle size, the smaller the significance of either problem. In the second case, the error will be proportional to the relative magnitude of the induced vortical motions and the square root of the granular temperature. Again, the induced motion depends on the pressure field and should be independent of particle size while the square root of the granular temperature varies proportionally to the particle size. Yet the scaled results plotted in figure 9 show no effect of particle size. Thus, one can infer that both effects are insignificant.

6. Conclusions

This paper has described measurements of the apparent thermal conductivity for a dry granular flow undergoing shear in an annular shear cell device. The results show that the bulk shear motion improves the internal transport of both heat and momentum and that both transport coefficients increase linearly with the imposed shear rate, indicating that similar internal mechanisms drive both transport processes. As the granular temperature varies as the square of the shear rate, the above results imply that both the conductivity and the viscosity enhancements are proportional to the square root of the granular temperature in much the same way as the kinetic theory of gases predicts that the viscosity and conductivity of a perfect gas are proportional to the square root of the thermodynamic temperature. This is a further indication that the granular temperature governs the internal transport processes in rapidly shearing granular flows and fulfils much the same role as the thermodynamic temperature in a gas.

However, there are differences in the internal mechanisms that lead to the

transport of heat and momentum. Momentum is transported both by particle collisions and by the random motion of particles through the bulk material. However, as heat transfer is a slow process, little heat can be conducted during the short duration of a collision and there is no analogue of the collisional mode for the heat transport. Consequently, at large particle concentrations, when the particles have limited free range of motion, there is almost no shear-induced enhancement of thermal conductivity. At the same time, the viscosity, working in the collisional mode, asymptotically approaches infinity as the solid concentration approaches the maximum value that can support a shear flow.

By comparing the results of tests on particles of various sizes and thermal properties, it was demonstrated that the thermal conductivity varies as:

$$k - k_0 = \rho_p c_p D_p^2 g(\nu) \frac{U}{H}, \tag{7.1}$$

where $g(\nu)$ is some function of the solid fraction ν. This provides the heat-transfer analogue to the famous prescription of Bagnold (1954) for the apparent viscosity:

$$\mu - \mu_0 = \rho_p D_p^2 f(\nu) \frac{U}{H}, \tag{7.2}$$

where $f(\nu)$ is another function of ν. Finally, we showed that the apparent Prandtl number for the shearing material is a function only of the solid fraction, further cementing the relationship between these two fundamental transport properties.

The authors would like to thank Igal Israeli for assisting in the design of the experimental apparatus, Herb Lloyd and John Yoshida for their masterful job of construction and Carver Mead, John Lee and Pierre Buckens for invaluable assistance in the design and construction of the transducers and associated electronics. This study was supported by the US National Science Foundation under grants MEA-8404415 and MEA-8352513 and the US Department of Energy under grant DE-FG22-88PC88913 for which the authors are extremely grateful. Special thanks are due to Holly Campbell for proofreading the manuscript and to Ian and Sean for pointing out the moon.

REFERENCES

BAGNOLD, R. A. 1954 Experiments on a gravity-free dispersion of large solid spheres in a Newtonian fluid under shear. *Proc. R. Soc. Lond.* A **225**, 49–63.

CAMPBELL, C. S. 1982 Shear flows of granular. Ph.D. thesis and *Rep.* E-200.7, California Institute of Technology.

CAMPBELL, C. S. 1986 Computer simulation of rapid granular flows In *Proc. 10th Natl Congr. of Applied Mechanics, Austin Texas, June 1986*, pp. 327–338. ASME.

CAMPBELL, C. S. 1989 The stress tensor for simple shear flow of a granular material. *J. Fluid Mech.* **203**, 449–473.

CAMPBELL, C. S. 1990 Rapid granular flows. *Ann. Rev. Fluid Mech.* **22**, 57–92.

CAMPBELL, C. S. & BRENNEN, C. E. 1985 Computer simulation of granular shear flows. *J. Fluid Mech.* **151**, 167–188.

CAMPBELL, C. S. & GONG, A. 1986 The stress tensor in a two-dimensional granular shear flow. *J. Fluid Mech.* **164**, 107–125.

CAMPBELL, C. S. & GONG, A. 1987 Boundary conditions for two-dimensional granular flows, In *Proc. Sino–US Intl Symp on Multiphase Flows, Hangzhou, China, August, 1987*, Vol. I, pp. 278–283. Zhejiang University Press, Hangzhou, China.

CAMPBELL, C. S. & WANG, G. D. 1986 The apparent conductivity of shearing particle flows. In *Proc. 8th Intl Heat Transfer Conf.*, vol. 4, pp. 2567–2572. Hemisphere.

CHUNG, Y. C. & LEAL, L. G. 1982 An experimental study of the apparent thermal conductivity of a sheared suspension of rigid spheres. *Intl J. Multiphase Flows* **8**, 605–625.

CRAIG, K., BUCKHOLTZ, R. H. & DOMOTO, G. 1987 The effects of shear surface boundaries on stresses for the rapid shear of dry powders. *Trans. ASME: J. Tribology* **109**, 232–237.

HANES, D. M. 1983 Studies on the mechanics of rapidly flowing granular-fluid materials. Ph.D. thesis, University of California, San Diego.

HANES, D. M. & INMAN, D. L. 1985 Observations of rapidly flowing granular-fluid materials. *J. Fluid Mech.* **150**, 357–380.

HUNT, M. L. & HSIAU, S. S. 1990 Thermal conductivity of granular flows. In *Proc. Intl 9th Heat Transfer Conf.*, pp. 177–182. Hemisphere.

LEAL, L. G. 1973 On the apparent conductivity of a dilute suspension of spherical drops in the limit of low particle Peclet number. *Chem. Engng Commun.* **1**, 21–31.

LIN, C. J., PEERY, J. H. & SCHOWALTER, W. R. 1970 Simple shear flow around a rigid sphere; inertial effects and suspension rheology. *J. Fluid Mech.* **4**, 1–17.

LÖFFELMANN, G. 1989 Theoretische und experimentelle Untersuchungen zur Schüttgut-Wand-Wechselwirkung und zum Mischen un Entmischen von Granulaten. Dr.-Ing. thesis, Universitat Fridericiana Karlsruhe (Technische Hochschule).

LUN, C. K. K., SAVAGE, S. B., JEFFREY, D. J. & CHEPURNIY, N. 1984 Kinetic theories for granular flow: inelastic particles in Couette flow and slightly inelastic particles in a general flow field. *J. Fluid Mech.* **140**, 223–256.

NIR, A. & ACRIVOS, A. 1976 The effective thermal conductivity of sheared suspensions. *J. Fluid Mech.* **78**, 33–48.

PATTON, J. S., SABERSKY, R. H. & BRENNEN, C. E. 1986 Convective heat transfer to rapidly flowing granular materials. *Intl J. Heat Mass Transfer* **29**, 1263–1269.

REYNOLDS, O. 1874 On the extent and action of the heating surface of steam boilers. *Proc. Lit. Phil. Soc. Manchester* **14**, 7–12. See also *Papers on Mechanical and Physical Subjects*, vol. 1, pp. 81–85. Cambridge University Press, 1900.

SAVAGE, S. B. & SAYED, M. 1983 Stresses developed by dry cohesionless granular materials in an annular shear cell. *J. Fluid Mech.* **142**, 391–430.

SUN, J. & CHEN, M. M. 1988 A theoretical analysis of heat transfer due to particle impact. *Intl J. Heat Mass Transfer* **31**, 969–975.

WALTON, O. R. & BRAUN, R. L. 1986*a* Viscosity and temperature calculations for shearing assemblies of inelastic, frictional disks. *J. Rheol.* **30**, 949–980.

WALTON, O. R. & BRAUN, R. L. 1986*b* Stress calculations for assemblies of inelastic spheres in uniform shear. *Acta Mechanica* **63**, 73–86.

WANG, D. G. 1991 Mechanics and heat transfer for granular flows. Ph.D. thesis, University of Southern California, Los Angeles.

WANG, D. G., SADHAL, S. S. & CAMPBELL, C. S. 1989 Particle rotation as a heat transfer mechanism. *Intl J. Heat Mass Transfer* **32**, 1413.

XAVIER, A. M. & DAVIDSON, J. F. 1985 Heat transfer in fluidized beds: convective heat transfer in fluidized beds. In *Fluidization* (ed. J. F. Davidson, R. Clift & D. Harrison). Academic.